Journal of Computational and Applied Mechanics, Vol. 3., No. 2., (2002), pp. 157–167

ON THE MULTIPLE SOLUTION OF AXISYMMETRIC MINIMUM SURFACES

Dóra H. Pálfalvi
PI-Hun Engineering Ltd.
33-34 Bem rkp., 1027 Budapest, Hungary
palfalvi.dora@pihun.hu

István Hegedűs
Department of Bridges and Structures, Budapest University of Technology and Economics
2 Bertalan Str., 1111 Budapest, Hungary
hegedus@vbt.bme.hu

[Received: April 28, 2002]

Abstract. The optimum condition for the unloaded shape of prestressed tents is met by minimum surfaces. The simplest type of such structures is a rotationally symmetric catenary surface. In this paper, the authors present an analysis which shows that catenary surfaces cannot fit arbitrarily chosen boundary circles of the tent, and also that if a solution of the problem exists, also a dual solution can be found.

Mathematical Subject Classification: 35J65, 49Q05
Keywords: optimum shape, minimum surface, envelope curve

1. Introduction

The problem about the existence and uniqueness of minimum surfaces under certain geometric constraints arose in connection with the optimum shapes of prestressed tents. The shape of a tent is considered optimum, if the fabric can be brought into a uniform stress state by prestressing.

In a previous paper [5] the mathematical background for the analysis of optimum shapes of tents with fixed boundaries has been published. It was shown that surfaces which meet the statical optimum condition are minimum surfaces as well. Also an iterative solution of the non-linear partial differential equation for the shape-function of membranes developing a self-stress state of uniform membrane forces has been presented. In certain cases the iteration proved divergent, which led to the analysis of conditions for the existence of the solution.

For the sake of simplicity, axisymmetric membranes will be dealt with. However, the nature of conditions for the existence of optimum shapes shows that they may also apply to other surfaces.

2. The shape of the meridian

In the case of axisymmetric membranes the problem of optimum shapes can be mathematically reduced to the analysis of the meridian. This analysis can be made analytically.

For an unloaded membrane of axisymmetric shape the following connection of the membrane forces and principal radii (principal curvatures) holds [1]:

$$\frac{N_\alpha}{R_\alpha} + \frac{N_\vartheta}{R_\vartheta} = 0, \tag{2.1}$$

where N_α, N_ϑ are the membrane forces in meridian and annular directions, and R_α, R_ϑ are the radii of curvatures in the same directions. These curvatures are the principal curvatures.

As the membrane of optimum shape develops a uniform tension self-stress state

$$N = N_\alpha = N_\vartheta\,.$$

Equation (2.1) leads to the geometric condition

$$\frac{1}{R_\alpha} = -\frac{1}{R_\vartheta}. \tag{2.2}$$

If the meridian of the surface is given as a function of z, i.e., in the form $r = r(z)$ then the principal curvatures can be expressed as

$$\frac{1}{R_\alpha} = \frac{r''}{\left[1+(r')^2\right]^{3/2}}, \qquad \frac{1}{R_\vartheta} = \frac{-1}{r\left[1+(r')^2\right]^{1/2}}, \tag{2.3}$$

where the differentiation with respect to z is denoted by $()'$.

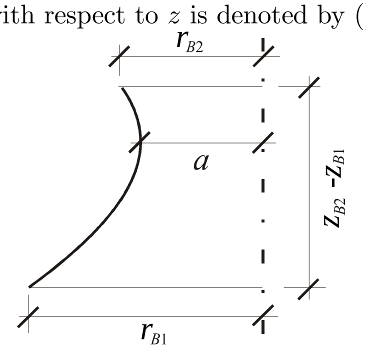

Figure 1. The meridian of the surface

Substituting equations (2.3) into equation (2.2), a non-linear second-order differential equation can be formed for r:

$$r''r - (r')^2 - 1 = 0\,. \tag{2.4}$$

The general solution of this differential equation is given in [3] as

$$r\,(z) = a\cosh\left(\frac{z-b}{a}\right), \tag{2.5}$$

where a and b are parameters of the solution. It follows from equation (2.5) that the meridians of rotationally symmetric membranes are *chain-curves*. The parameter 'a' can be interpreted as the radius of the throat circle of the catenoid surface (Figure 1) (or the height of the deep point of the chain-curve) while 'b' is its distance from the $z = 0$ co-ordinate plane.

If the levels z_{B1}, z_{B2} and the radii r_{B1}, r_{B2} of the boundary circles are given values (Figure 1), the real parameters a and b have to be calculated by solving the conditional equation system:

$$r_{B1} = a \cosh\left(\frac{z_{B1} - b}{a}\right), \qquad r_{B2} = a \cosh\left(\frac{z_{B2} - b}{a}\right). \tag{2.6}$$

We have found, on the one hand, that the above equation system does not always have a real solution for the parameters a and b, and, on the other hand, if there exist a pair of real numbers for a and b which fulfill the equation system, then another pair of a and b can be found. These facts give rise to two questions: one, which conditions decide that the mechanical problem has or does not have any solution, and another, which of the multiple mathematical solutions is the real solution for the mechanical problem.

In the subsequent sections, first, conditions for the existence of the solution will be dealt with, then the minimum property of the surfaces obtained by the multiple mathematical solutions will be checked.

3. **The envelope of chain-curves intersecting at a common point**

On the basis of the general solution of equation (2.5) a transformed form can be derived which makes analyzing our problem easier. First, let r/a be replaced by ρ, z/a by ζ, b/a by β, then let a common multiplier coshβ of ρ and ζ be introduced into the general solution. In this way we can arrive at the equation

$$\rho\,(\zeta, \beta) = \frac{1}{\cosh\beta} \cosh\left(\zeta \cosh\beta - \beta\right) . \tag{3.1}$$

This form makes analyzing our problem easier because one of the boundary points of the meridian always gets to the point $\zeta = 0$, $\rho = 1$. Setting parameter β to different values, equation (3.1) generates a set of chain-curves passing through that common point – see Figure 2. The problem of fitting a chain-curve to the points with co-ordinates (z_{B1}, r_{B1}) and (z_{B2}, r_{B2}) can be transformed to that of selecting chain-curves from the set generated by equation (3.1), which passes through the point of the co-ordinates

$$\zeta_B = \frac{z_{B2} - z_{B1}}{r_{B1}}, \quad \rho_B = \frac{r_{B2}}{r_{B1}} . \tag{3.2}$$

A glance at the diagram of the series of chain-curves generated by equation (3.1) (see Figure 2) makes it obvious that there is an envelope which divides the co-ordinate plane (ζ, ρ) into a part where points cannot be reached by chain-curves passing through the point (0,1), and another part, where it is possible. Figure 2 also shows the shape of the envelope resembles a shifted chain-curve $\rho = \cosh\zeta - 1$, however, it must differ from that curve because the envelope has to get closer to the diagram of $\rho = \cosh\zeta$ if ζ has a larger absolute value.

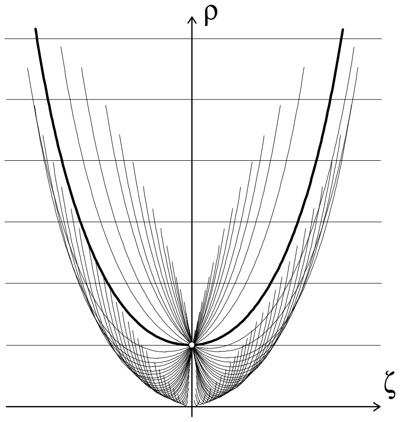

Figure 2. Chain-curves passing through the point $(0, 1)$

The equation of the envelope of the series of curves generated by a parametric equation is determined by the conditions that points of the envelope are also points of those curves touching the envelope, and the first order variation of the parametric equation with respect to its parameter must vanish at the touching points. These two conditions can be expressed as

$$F(\rho, \zeta, \beta) = 0\,, \tag{3.3}$$

$$\frac{\partial F(\rho, \zeta, \beta)}{\partial \beta} = 0 \tag{3.4}$$

where equation (3.3) is the equation of the curves with parameter β. The equation of the envelope can be obtained by eliminating β from equations (3.3) and (3.4) [4].

In our case $F(\rho, \zeta, \beta)$ is the same as equation (3.1) arranged to zero, conditions (3.3) and (3.4) yield a system of transcendent equations as follows:

$$\rho\cosh\beta - \cosh(\zeta\cosh\beta - \beta) = 0\,, \tag{3.5}$$

$$\rho\sinh\beta - \sinh(\zeta\cosh\beta - \beta)(\zeta\sinh\beta - 1) = 0\,. \tag{3.6}$$

Though β cannot be analytically eliminated from the above equation system, the envelope can be plotted point by point using numerical solutions of equations (3.5) and (3.6) for different values of β.

The plot of the envelope is the continuous line in Figure 3. For small values of ζ its shape seems to osculate the curve of the function $\rho = \cosh\zeta - 1$, which is shown with dashed line in Figure 3.

However, for large values of β, the numerical solutions of equations (3.5) and (3.6) are getting more and more inaccurate and they do not permit us even to settle the question whether the envelope starts with a zero or nonzero slope at the origin.

This question can be answered by analyzing the curve of the deep points of the chain-curves in Figure 2. Co-ordinates of the deep points of chain-curves passing

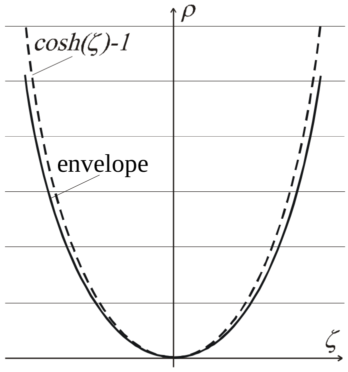

Figure 3. The envelope curve

through the point $(0, 1)$ are

$$\rho_0 = \frac{1}{\cosh \beta} \qquad \zeta_0 = \frac{\beta}{\cosh \beta} .$$

These expressions permit us to eliminate parameter β and to express the equation of the curve of the deep points as

$$\zeta_0 = \rho_0 \cdot \operatorname{arccosh} \frac{1}{\rho_0} . \tag{3.7}$$

Though equation (3.7) cannot be made explicit for ρ_0, it enables us to answer whether the curve of the deep points starts with a zero or with nonzero slope from the origin. Producing the first derivative of equation (3.7) as

$$\frac{\mathrm{d}\,\zeta_0}{\mathrm{d}\,\rho_0} = \operatorname{arccosh} \frac{1}{\rho_0} - \frac{1}{\rho_0 \cdot \sqrt{1-\rho_0^2}} ,$$

then performing the limit transition for its reciprocal at $\rho_0 = 0$, we find

$$\lim_{\rho_0 \to 0} \left(\frac{\mathrm{d}\,\zeta_0}{\mathrm{d}\,\rho_0} \right)^{-1} = 0,$$

which means that the curve starts with a zero slope.

Since the deep points of the chain-curves are above the envelope curve, if the curve of the deep points starts with a zero slope at the origin, the envelope does the same.

Again the diagram of the chain-curves generated by equation (3.1) shows that each point (ζ_B, ρ_B) of the domain of possible solutions is a point of intersection of two curves of the series, that is, if we have a solution of our problem, we always have a dual solution as well. If the point (ζ_B, ρ_B) is exactly on the envelope curve, then the two meridians coincide.

The domain of the possible solutions can be divided into a part (A), where the deep points of the intersecting chain-curves lie on different sides of the co-ordinate plane split by axis ρ, and another part (B), where the deep points lie on the same side

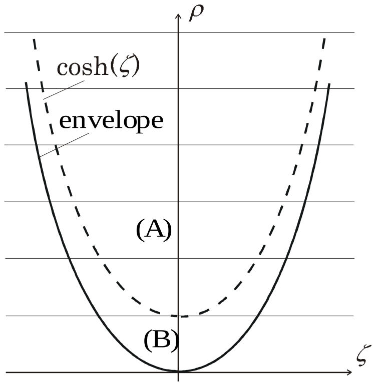

Figure 4. Two regions of the domain of solutions

The two regions are separated by the chain-curve the deep point of which lies on axis ρ (Figure 4). Since we could not derive a closed formula for the envelope, its shape can be analyzed only numerically. The approximate formula

$$\mathrm{Env}\zeta \approx \cosh\zeta - 1$$

yields fairly good first estimates both for small values of ρ and for larger values as well. For values of ζ larger than about 0.7 we find a more accurate envelope by assuming that the condition

$$\frac{\mathrm{d}\,\mathrm{Env}(\zeta_e)}{\mathrm{d}\zeta_e} = \frac{\mathrm{d}\,F(\rho_e, \zeta_e, \beta)}{\mathrm{d}\zeta_e}$$

holds for the first estimate, where the index e refers to the place of the envelope. In this way we can write

$$\sinh\zeta_e \approx \sinh(\zeta_e \cosh\beta - \beta)\,,$$

which permits us to approximate ζ_e in the form

$$\zeta_e \approx \frac{\beta}{\cosh\beta - 1}, \tag{3.8}$$

and then the corresponding ρ_e as

$$\rho_e = \frac{1}{\cosh\beta}\cosh\left(\frac{1}{\cosh\beta - 1}\right). \tag{3.9}$$

In Figure 5 the plots of the first estimate (dashed line) and the refined envelope calculated using equations (3.8) and (3.9) are shown

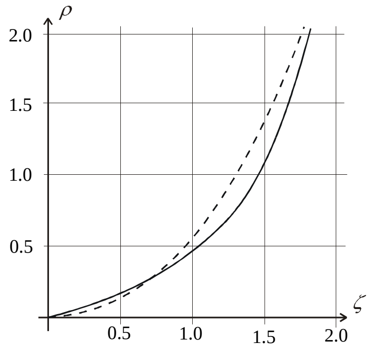

Figure 5. Approximate envelopes

The envelope gives an answer to our first question: the data of the boundaries determine that in the given geometrical case a membrane with optimum shape does or does not exist. For any pairs of the radii of the boundary rings there exists a maximum value of height of the surface that permits us to connect the rings with a surface of optimal shape. If the height is less than this value, we can find two surfaces which meet the optimum condition, if the height is chosen bigger than this value, we cannot find solutions.

4. **The minimum surface**

It was shown in [5] that the surface of the optimum shape of unloaded membranes is minimum. However, in the last section two solutions were found for the optimum shape. This result raises the problem: which curve specifies the minimum-surface and what extreme property the other curve exhibits.

To answer this question two types of numerical investigation were performed.

First we shall consider a combination of the two solutions.

Let the functions of the curves passing through an arbitrarily chosen point within the envelope be called $\rho_1(\zeta)$ and $\rho_2(\zeta)$. Let $\rho_1(\zeta)$ belong to the curve which runs higher between the points of intersection than the other curve.

The curves representing the function

$$\rho_\alpha(\alpha, \zeta) = \alpha\ \rho_1 + (1 - \alpha\ )\ \rho_2$$

also pass through the end points of the curves belonging to $\rho_1(\zeta)$ and $\rho_2(\zeta)$. If $\alpha = 1$, then $\rho_\alpha(\zeta) = \rho_1(\zeta)$, if $\alpha = 0$, then $\rho_\alpha(\zeta) = \rho_2(\zeta)$, if $0 < \alpha < 1$, then the curve of $\rho_\alpha(\zeta)$ lies between that of $\rho_1(\zeta)$ and $\rho_2(\zeta)$.

The area $A(\alpha)$ of the surface assigned by $\rho_\alpha(\alpha, \zeta)$ can be analytically expressed as a fairly complicated definite integral. Instead of using this integral, we numerically calculated the surface area for some values of α, and then plotted the results.

Figure 6 shows a typical plot of $A(\alpha)$. In this case co-ordinates ζ of the deep points of the curves have the same sign, however, plots belonging meridians with deep points that lie at values of ζ with different signs show the same characteristics. The plots clearly show that meridians at $\alpha = 1$ result in local minima of surface areas, and at $\alpha = 0$ in their local maxima. Hence, meridians $\rho_1(\zeta)$ can be stable solutions, but $\rho_2(\zeta)$ are always unstable ones.

It may cause difficulties to explain that at certain negative values of α the computed surface area gets lower than the minimum at $\alpha = 1$. The reason may be that the combined meridians do not always characterize surfaces with a physically realistic surface. If the meridian intersects the axis of rotation, between the points of intersection the integral takes into account a negative surface area. However, the plots of the meridians show that in some cases the area of the combined surface can get smaller

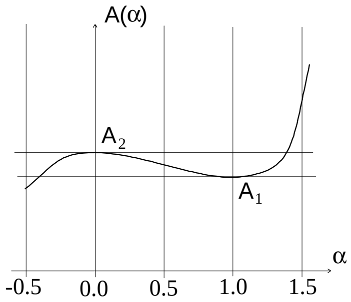

Figure 6. The plot of $A(\alpha)$

than the local minimum before this intersection happens. To clarify this unexpected result, an individual analysis of the extreme properties of the surfaces was performed.

Secondly, we consider a variation of different functions.

The extreme property of the meridians $\rho_1(\zeta)$ and $\rho_2(\zeta)$ can be individually investigated by a numerical variational analysis. For that purpose we have to choose functions which take zero values at the boundaries like

$$\delta\rho = \zeta\ (\zeta_B - \zeta)\,,$$
$$\delta\rho = \sin\left(\frac{\pi\,\zeta}{\zeta_B}\right),$$
$$\delta\rho = \cosh\left(\zeta - \frac{\zeta_B}{2}\right) - \cosh\left(\frac{\zeta_B}{2}\right),$$

and to use them to vary the meridians and the surfaces. By adding $\varepsilon\,\delta\rho$ to functions $\rho_1(\zeta)$ and $\rho_2(\zeta)$ we can numerically calculate the surface area

$$A(\rho_1) + \delta A(\rho_1) = A(\rho_1 + \varepsilon\,\delta\rho),$$
$$A(\rho_2) + \delta A(\rho_2) = A(\rho_2 + \varepsilon\,\delta\rho)$$

for different values of ε, then plot the results in a common co-ordinate system.

Figure 7 shows some characteristic results of the analysis made in this way. On the left hand-side of Figure 7 the variation of the surface area is shown for a pair of meridians fitting the same boundary points. Plots A_1 and A_2 clearly show that both

$A(\rho_1)$ and $A(\rho_2)$ have local extreme values at $\varepsilon = 0$. That is, both $A(\rho_1)$ and $A(\rho_2)$ are extremals of the numeric variational problem, because their first order variation is zero. On the other hand, $A(\rho_1)$ has a local minimum and $A(\rho_2)$ also has a local maximum at $\varepsilon = 0$, which means, their second order variations are differently signed. This difference indicates different extreme properties: the surface which belongs to ρ_1 is a stable minimum surface, while the other is unstable.

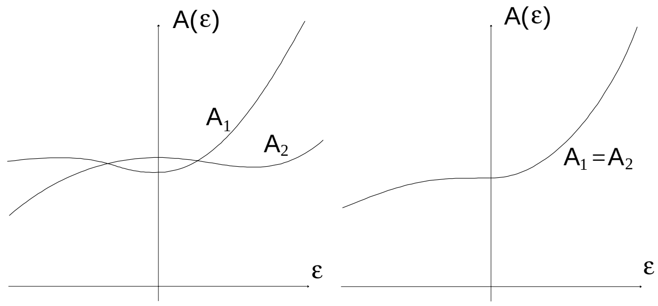

Figure 7. Variation of surface areas

On the right-hand side of Figure 7 the variation of the surface area is shown which belongs to coinciding meridians $\rho_1 = \rho_2$. In this case both the first and second order variations are zero and the surface assigned by the meridians is at the limit of the stability.

The plots again show that the condition stated by equation (2.4) for axisymmetric minimum surfaces is not a global minimum condition. It can be met by surfaces which are locally minimum surfaces and also by surfaces which are not minimum surfaces at all. Moreover, it may happen that the area of the varied surface is smaller than that of the minimum surface.

5. **Connection with the areas of the boundary rings**

If we neglect the small effect of gravity, the shape of soap films stretched between concentric circular boundary rings is an annular plate, which turns into a catenoid shaped minimum surface if the planes of the boundary rings get separated. Experiments with such soap films can be used to check the results of the above analysis. Sometimes they show an interesting phenomenon: by increasing the distance of the rings, the catenoid gets more and more laced, and at a certain distance it snaps into two separate circular plates stretched on the two boundary rings.

This snapping is usually explained by the reasoning that the catenoid snaps into separate circles when its area gets equal to the sum of the area of the two circles. However, the existence of axisymmetric surfaces with a smaller area than the stable minimum surface and also the local nature of the minimum property of minimum surfaces give rise to serious doubts about the tenability of that reasoning.

Our results can also be used to settle this problem. The area of the catenoid surfaces generated by equation (3.1) can be analytically expressed as

$$A(\zeta_B, \beta) = \frac{2\pi}{\cosh^2 \beta} \int_0^{\zeta_B} \cosh^2(\zeta \cdot \cosh\beta - \beta)\, \mathrm{d}\zeta \, \cosh\beta =$$

$$= \frac{\pi}{\cosh^2 \beta} \left[\frac{\sinh 2(\zeta_B \cdot \cosh\beta - \beta)}{2} + (\zeta_B \cdot \cosh\beta - \beta) \right]$$

and $A(\zeta_B, \beta)$ can be matched with the sum of the area of the boundary rings

$$A_R(\zeta_B, \beta) = \pi \left[\frac{\cosh^2(\zeta_B \cdot \cosh\beta - \beta)}{\cosh^2 \beta} + 1 \right]$$

Parameters, when $A(\zeta_B, \beta) = A_R(\zeta_B, \beta)$, specify pairs of coordinates ζ_B and ρ_B of boundary circles of our interest

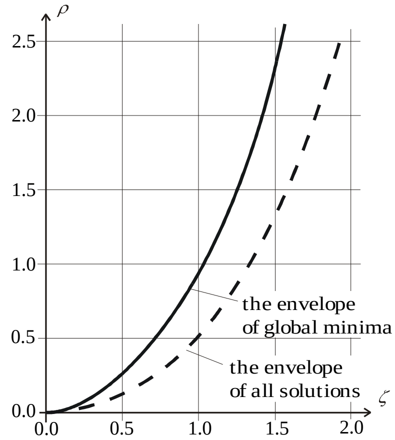

Figure 8. The envelope of global minima

In Figure 8 a continuous line represents the boundary points of those meridians for which the area of the stable minimum surface is equal to the sum of the areas of their boundary circles. The first (and everywhere conservative) estimate of the envelope is also plotted (dashed line). The figure shows that the two curves permit solutions of the rotationally symmetric minimum surface problem, where the area of the minimum surface is larger than the sum of area of the boundary circles.

The continuous line can also be considered as an envelope. If the points within the continuous line are connected to the point (0,1) by chain-curves we obtain minimum surfaces with globally minimum surface area.

6. **Conclusions**

The analysis has shown that the differential equation for the meridian of axisymmetric minimum surfaces cannot be solved for arbitrary values of the boundary radii and if a solution can be found, also a dual solution exists, unless the two solutions coincide. It means that in typical cases, besides the minimum surface, another surface of revolution exists, which also develops uniform self-stress state. Both surfaces are catenary surfaces, but the area of the minimum surface behaves as a minimum, while that of the dual solution behaves as a maximum against small variations. In case of coinciding solutions only stationarity can be found.

Both minimum and maximum properties are of local nature. It is quite obvious for the surface maximum, but more or less unexpected for the minimum surface, because in case of appropriate values of radii and distance of boundary circles, the area of the minimum surface is larger than that of properly chosen surfaces fitting the same boundaries. The analysis has also clarified under what conditions the area of the minimum surface is the global minimum of the problem.

These results make it clear why does the stability of our iterative method depend both on the geometrical data, and on the mesh of the discretizing net and why does it also exhibit the same sensibility in any minimum surface problems characterized by two or more boundary curves. Similarly to the catenary surface problem, the existence of these surfaces is also conditioned by the data of the boundaries and the solutions are multiple solutions as well. The closer the multiple solutions are to each other the poorer the stability of the iterative solution is. Refinement of the mesh does not only improves the solution but also makes the iteration more stable because it decreases the chance to drop from a convergent path into a closely divergent one.

Acknowledgement. Investigations that constitute the basis of the present study were parts of research programs OTKA T032057 and FKFP 0391/1997 supported by the Hungarian Academy of Sciences and the Hungarian Ministry of Education. The authors express sincere thanks for their support.

REFERENCES

1. Hegedűs, I.: *Shell structures*, Műegyetemi Kiadó, Budapest, 1998. (in Hungarian)
2. H. Pálfalvi, D. and Hegedűs, I.: *About the shape of the meridian of rotationally symmetric tent structure*, A BME Hidak és Szerkezetek Tanszéke Tudományos Közleményei, HU ISSN 1586-7196, (2001), 63-70. (in Hungarian)
3. Kamke, E.: *Differentialgleichungen I., Gewöhnliche Differentialgleichungen*, Akademische Verlagsgesellschaft, Leipzig, 1967.
4. Korn, G.A. and Korn, T.M.: *Mathematical Handbook for Scientists and Engineers*, McGraw-Hill, New York, 1968.
5. Pálfalvi, D. and Hegedűs, I.: *On the statical problems for determination of the shape of prestressed tents*, Periodica Polytechnica Ser. Civ. Eng., **42**(2), (1998), 161-169.